

Effects of Parameters on Inhomogeneous Deformation and Damage in Isothermal Local Loading Forming of Ti-Alloy Component

Zhichao Sun, He Yang, and Nianguang Sun

(Submitted September 13, 2010; in revised form January 22, 2011)

Isothermal local loading (ILL) forming technology provides a new way to form largescale rib-web (LSRW) components of Ti-alloy, widely used in the aero-space fields as key load-bearing structures. However, the metal undergoes complex plastic inhomogeneous deformation and microstructural evolution, this will lead to macroscopical forming defects and further damage due to multi-process parameters and local loading method, making the process and forming quality hard to control. Using numerical simulation, combined with experiment, influences of various process parameters on forming process, inhomogeneous deformation and damage have been explored for ILL of LSRW components, such as the types of die-forging mode, frictional conditions, and local loading parameters (partitioning of the loading zone, constraint conditions, and loading pass). Then the reasonable forming conditions for LSRW components of Ti-alloy to be studied are proposed. The practical forming experiment of TA15 LSRW component was achieved successfully and the forging with good forming quality, excellent microstructure, and comprehensive mechanical properties was obtained, which indicates the reliability and practical value of results obtained in this article.

Keywords isothermal local loading, largescale rib-web component, numerical simulation, process parameters

1. Introduction

Isothermal local loading (ILL) forming technology, in which load is applied to part of the billet and the component is formed by changing the loading zones, provides a new way to form largescale rib-web (LSRW) components of Ti-alloy, which are widely used in the aero-space fields as key load-bearing structures under severe working conditions (Ref 1, 2). Therefore, the macroscopical forming precision, microstructure and mechanical properties of such component must be strictly controlled. However, the ILL forming of large-scale component is complicated and the process is difficult to carry out one side due to the complexity in shape, difficult-to-deformation materials material used, on the other side due to the presence of coupling effects of multi-fields and multi-factors as well as the alternation between loading zone, unloading zone, and transitional region (Ref 3). The metal undergoes complex plastic inhomogeneous deformation and microstructural evolution, which will not only lead to some macroscopical forming defects, such as shift, rib-piercing, and streamline foul-up, from which further damage is prone to occur (Ref 4-6), but also

result in bad microstructure and poor performance. The forming process, inhomogeneous deformation and possible damage, as well as microstructure and mechanical properties of the component are determined by hot working conditions such as die-forging mode, friction, and local loading parameters (partitioning of loading zone, constraint conditions, and loading pass).

So analyzing the inhomogeneous deformation behavior and possible damage and revealing the process parameters' effects are the key problems for the application and development of ILL forming technology. Some work has been done for integral isothermal forging of small Ti-alloy components (Ref 7-9). The forming process, possible defects, and mechanism of unequal deformation during ILL forming of annular ti-alloy component were studied, and it was found that the underfill and streamline foul-up could be improved using the billet with unequal thickness (Ref 3, 5, 6). The influence of billet thickness on the forming quality of TA15 bulkhead isothermal forming was discussed and the two loading modes (integral loading and local loading) were compared (Ref 10). An analogue experiment using square billets to study the effects of local loading conditions on the microstructure and mechanical properties of TA15 Ti-alloy workpieces was designed (Ref 11). The effect of deformation inhomogeneity on the microstructure and mechanical properties of LSRW component of Ti-alloy under local loading forming was discussed (Ref 12).

While a lack of understanding of the process parameters and their effects on complex LSRW component ILL forming processes persists. So in this article, the process of complex LSRW component ILL forming and the parameters on it are investigated using numerical simulations, combined with experiment for further process and parameters optimization.

Zhichao Sun, He Yang, and Nianguang Sun, State Key Lab of Solidification Processing, Department of Materials Science and Engineering, Northwestern Polytechnical University, P.O. Box 542, Xi'an 710072 Shaanxi, People's Republic of China. Contact e-mail: yanghe@nwpu.edu.cn.

2. FE Modeling for Rib-Web Component ILL and Engineering Application Verification

Figure 1 shows the configuration of a typical LSRW component. Figure 2 shows the rigid-plastic FE model for a local loading process based on DEFORM-3D platform. Two kinds of lower dies (as shown in Fig. 3) are adopted corresponding to flashless die forging and open-die forging processes. To implement the local loading process, two combined upper dies are used, namely Top die 1 and Top die 2 (Fig. 2), corresponding to the partitioning of the loading zones in the billet.

The material of the billet used is TA15 (Ti-6Al-2Zr-1Mo-1V) Ti-alloy, and its macroscopic constitutive relationship was determined by stepwise regression model developed by authors as follows (Ref 13):

$$\ln \sigma = \begin{cases} -30.7 + 7.20 \times 10^3 T^{-1} + 0.526 \ln \dot{\epsilon} - 3.47 \times 10^7 T^{-2} \\ -430 T^{-1} \ln \dot{\epsilon} - 6.00 \times 10^{-3} \ln^2 \dot{\epsilon} - 587 T^{-1} \epsilon & (\epsilon < 0.75) \\ -4.41 + 1.07 \times 10^4 T^{-1} + 0.450 \ln \dot{\epsilon} \\ -5.00 \times 10^{-3} \ln^2 \dot{\epsilon} - 315 T^{-1} \ln \dot{\epsilon} & (\epsilon \geq 0.75) \end{cases} \quad (\text{Eq 1})$$

where σ is the flow stress (MPa), T absolute deformation temperature (K), $\dot{\epsilon}$ plastic strain rate (s^{-1}), ϵ is the plastic strain.

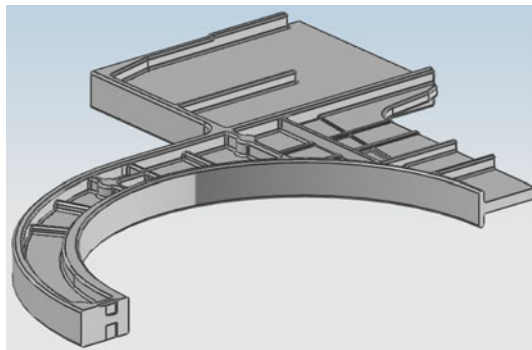


Fig. 1 Geometrical model of large-scale complex component

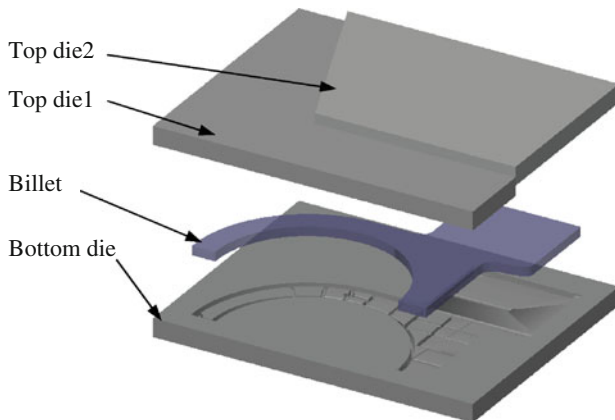


Fig. 2 FE model of local loading forming

The local loading process mentioned in this article consists of one or more loading passes and each loading pass includes two loading steps. In step 1, Top die 1 is loaded while Top die 2 is fixed as a constraint; in step 2, Top die 2 is loaded and Top die 1 is fixed as a constraint template. After all loading passes are completed, according to requirement a refining step may be considered by loading both Top die 1 and Top die 2 simultaneously.

The practical forming experiment of a typical TA15 large component by local loading was done to verify the FE model developed. During the experiment and FE simulation the same process conditions were adopted as follows: material of billet was TA15 Ti-alloy, initial thickness of billet was 50 mm, forming temperature of billet and die was 970 °C, loading speed of upper die was 0.1 mm/s, and total reduction amount was 35.5 mm (reduction of local loading was 34 mm, reduction of refined forming was 1.5 mm), flashless die forging mode was used and upper die was partitioned along the rib of component, single-pass local loading was adopted, glass-based lubricant was used. Figures 4 and 5 show the simulation and experimental results of different forming stages. It can be found that the simulation results agree well with experimental ones, so the FE model developed can be used for the process simulation and analysis.

3. Simulation Conditions and Definition of Object Parameters

Numerous simulations were done for LSRW component ILL forming by changing local loading conditions including the types of die-forging mode, frictional conditions, and local loading parameters (partitioning of the loading zone, constraint conditions, and loading pass).

Initial thickness of billet is 50 mm, forming temperature of billet and die is 970 °C, loading speed of upper die is 0.1 mm/s, and total reduction amount is 35.5 mm. Two types of die forging mode, open-die forging and flashless die forging are adopted. Values of frictional factor m are taken to be 0.1, 0.3, 0.5;

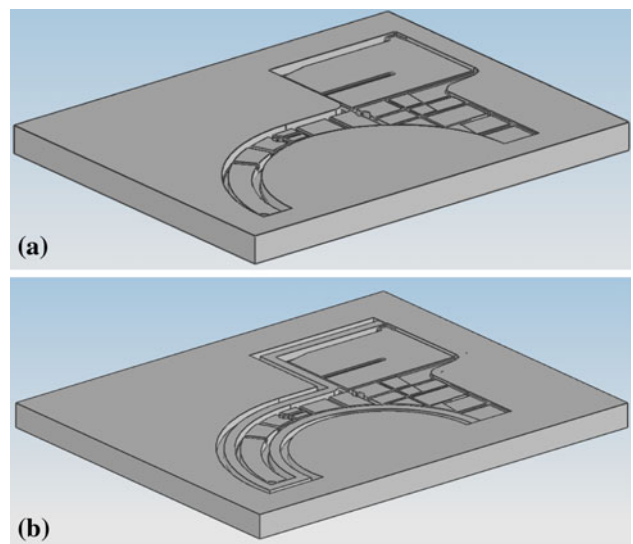


Fig. 3 Geometrical model of lower die: (a) under flashless die forging and (b) open-die forging

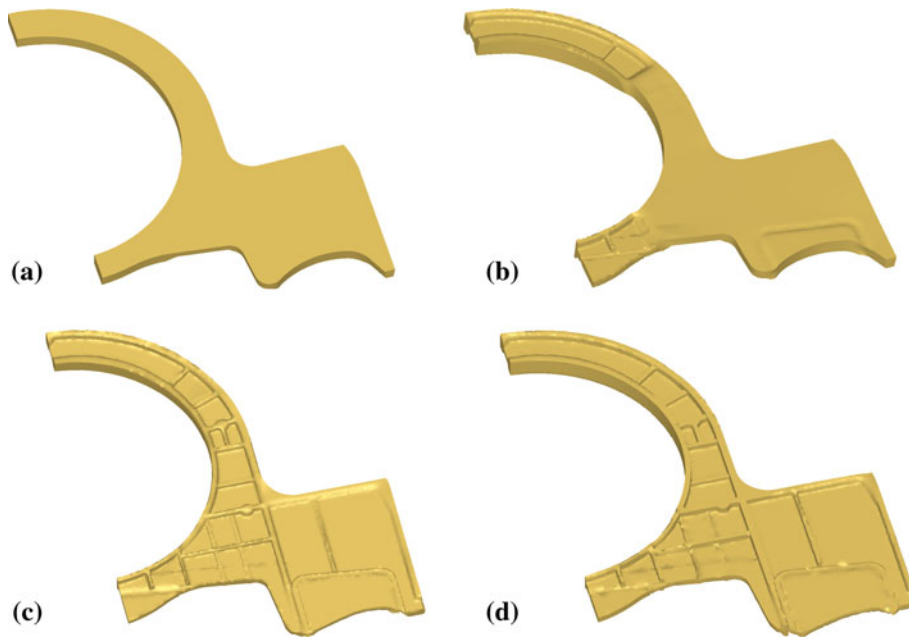


Fig. 4 Shape of workpiece during single-pass isothermal local loading forming by simulation: (a) initial billet, (b) after first local loading step, (c) after second local loading step, and (d) after refined forming step

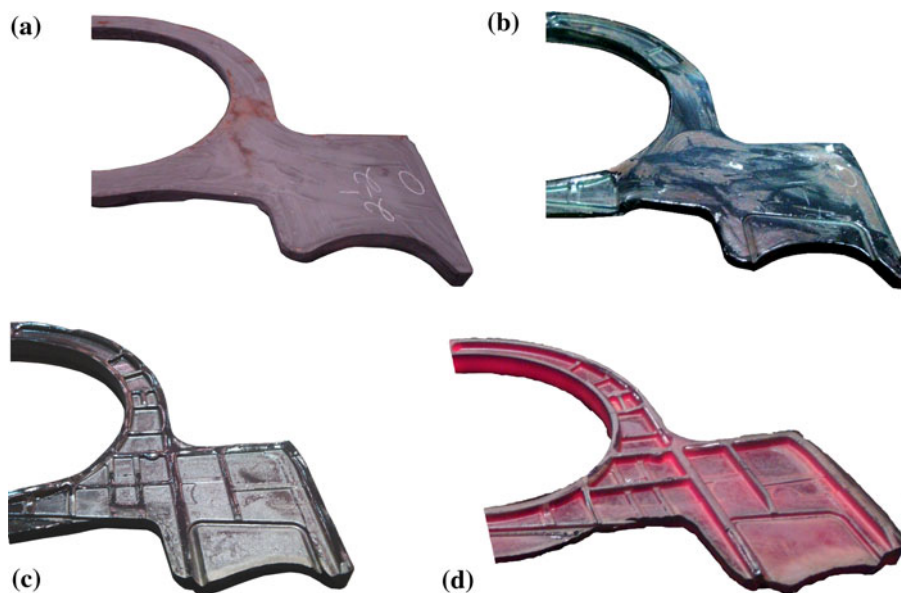


Fig. 5 Results of TA15 large component forming experiment by single-pass isothermal local loading: (a) initial billet, (b) after first local loading step of first pass, (c) after second local loading step of first pass, and (d) forging after second loading pass

constraint clearances are taken to be 0.5, 1.0, 1.5, 2.0 mm. For a single-pass loading forming mode, Top die 1 is loaded with a forming reduction of 34 mm while Top die 2 is maintained as a constraint template with constraint clearance of 1 mm. In the second loading step, loadings from upper dies are swapped. Top die 2 is loaded with a forming reduction of 34 mm, while Top die 1 is maintained as constraint template with constraint clearance of 1 mm. Finally, the two dies are both loaded and refined forming is performed with a reduction 1.5 mm after local loading. For a two-pass loading forming mode, reduction

per loading pass is 17.0 mm, and for fine deformation the reduction amount is 1.5 mm.

If without special statement in what follows only the single-pass loading forming process will be discussed.

During hot working of Ti-alloy the inhomogeneous deformation and tensile stress in local zone will lead to damage. Croft-Latham (C&L) damage criterion (Ref 14) described this phenomenon and which was applied successfully to predict the cracking of Ti-alloy in hot working process (Ref 15). The damage factor is defined as $D_f = \int \frac{\sigma^*}{\sigma} d\epsilon$, where σ^* is the

maximum tension stress, σ is the equivalent stress, and $d\epsilon$ is the incremental of equivalent strain. Here, the damage factor D_f is used to describe the possibility of damage. When the damage factor is large when compared to the critical value, cracks may generate, and damage will occur.

The average equivalent strain and its standard deviation are adopted to evaluate the degree and uniformity of deformation. The larger is the degree of deformation uniformity, or the smaller the standard deviation, the better is the forming quality.

4. Effects of Die Forging Modes on Inhomogeneous Deformation and Damage

There are two modes of die forging, open-die forging and flashless die forging, according to whether flash is employed or not. Here, two kinds of dies are designed to analyze the effect of these two forging modes on the forming process and quality. Figure 6 shows the distribution of equivalent strain under these two forging modes. With all other forming parameters considered constant, the average equivalent strain for open-die forging is 0.803 with standard deviation of 0.279 (deformation of the flash is not considered), while for flashless die forging the average equivalent strain is 0.842 with standard deviation of 0.281. Thus, with flashless die forging the deformation degree of the billet is slightly larger than that by open-die forging.

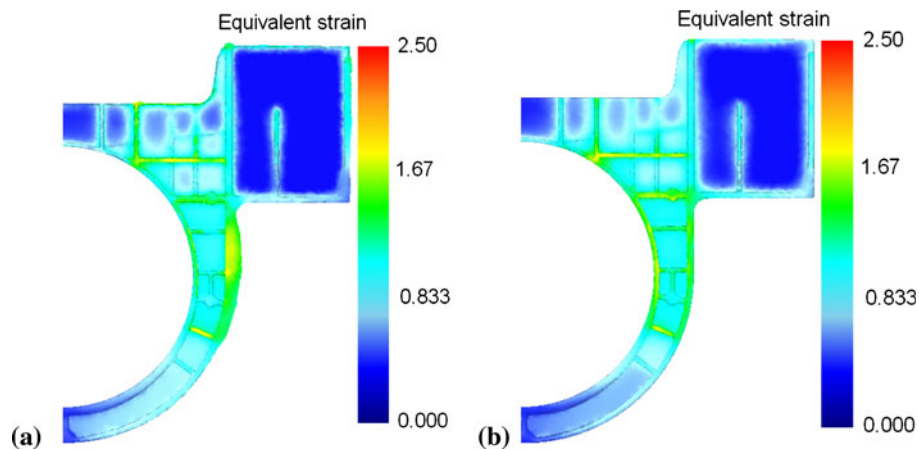


Fig. 6 Distribution of equivalent strain under different die forging modes: (a) open-die forging and (b) flashless die forging

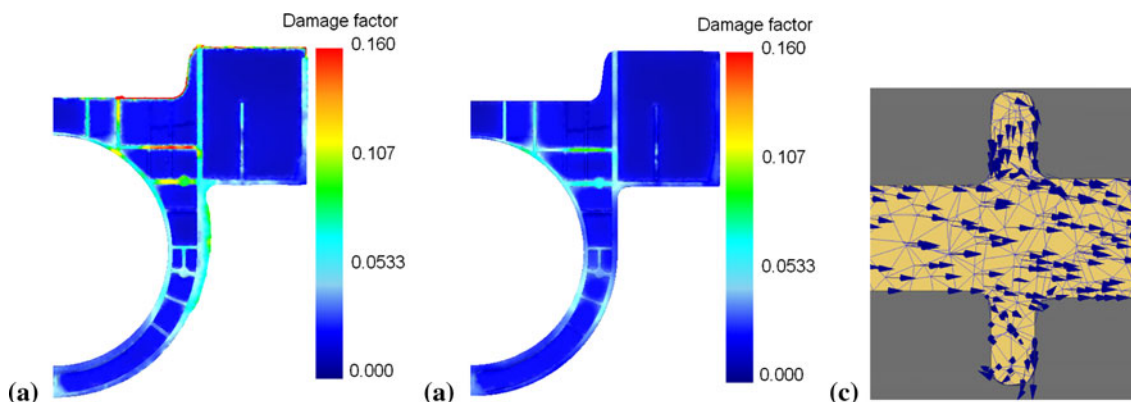


Fig. 7 Damage factor under different die forging modes: (a) open-die forging, (b) flashless die forging, and (c) schematic diagram of piercing rib

Figure 7 shows the possibility of damage that may occur under these two forging modes. For open-die forging, the mean damage factor D_f is 0.0354, while it is 0.0285 for flashless die forging. Under open-die forging, the regions with large damage factors are along the transverse ribs as shown in Fig. 7(a), and the transverse flows of metal will result in “rib-piercing” as shown in Fig. 7(c).

The damage factor under open-die forging is more extensive than that under flashless die forging because during the second loading step, Top die 2 loading, the metal flows more easily toward unloading zones due to the existing of die flash, thus piercing of the transverse ribs may occur. The forming load under flashless die forging is slightly larger, while transverse flow of metal resulting in “rib-piercing” can be avoided, as indicated by lower damage factors. Thus, for this forming process, flashless die forging is preferable and in what follows only this mode of forging will be discussed.

5. Frictional Effects on Inhomogeneous Deformation and Damage

Friction conditions affect not only the forming load and abrasion of the die but also the radial filling of metal, i.e., the equilibrium of deformation. To describe these frictional effects between the billet and the dies, a constant shearing friction

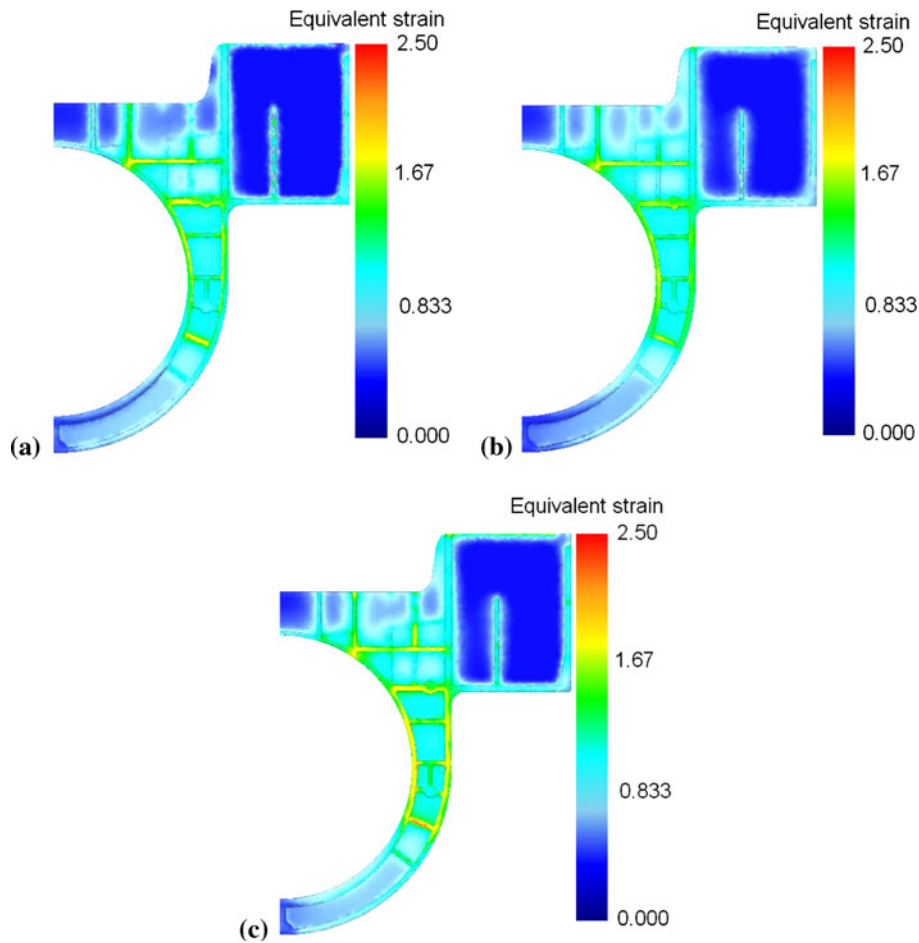


Fig. 8 Distribution of equivalent strain: (a) $m = 0.1$, (b) $m = 0.3$, and (c) $m = 0.5$

model is used wherein values frictional factor are chosen to be 0.1, 0.3, 0.5. With all other forming parameters considered constant, the average equivalent strain is 0.811 for $m = 0.1$ with standard deviation of 0.272 (Fig. 8a); for $m = 0.3$ the average equivalent strain is 0.842 with standard deviation 0.281 (Fig. 8b); and for $m = 0.5$ the average equivalent strain is 0.867 with standard deviation 0.308 (Fig. 8c). Friction conditions have little effect on distributions of equivalent strain of billet, while with the increase of friction factor the average equivalent strain of billet increases, and the uniformity of deformation reduces due to the metal flow weakening on the surface of billet.

6. Effect of Local Loading Conditions on Inhomogeneous Deformation and Damage

6.1 Partitions of Loading Zone

The billet is divided into two zones for local loading. During each local loading step only one zone is loaded, the other parts of the billet, the transitional zone, and constraint zone, constitute the unloading zone. The whole billet can be partitioned along the rib or on the web according to the corresponding positioning of the partition borderline on the billet. Figure 9 sketches two partition modes. During local loading process there exists a fitting clearance between the top

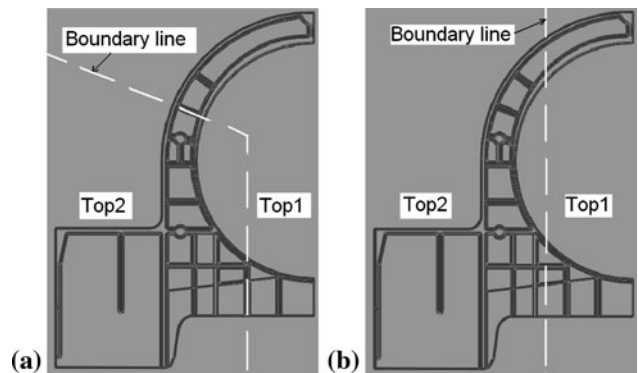


Fig. 9 Schematic diagram of partition mode: (a) partition along the rib and (b) partition on web

dies. If partitioned on the web, burring may occur in the transitional zone as shown in Fig. 10(a), and the metal here undergoes shearing deformation, which is not advantageous from a forming quality perspective. If partitioned along the rib, some metal will aggregate here in advance, and will be beneficial in filling the rib, while burring may thus be avoided, as shown in Fig. 10(b).

Figure 11(a) shows the distribution of equivalent strain when partitioned on the web. After forming, the average equivalent strain is 0.880 with standard deviation of 0.320.

When partitioned along the rib, the average equivalent strain is 0.842 with standard deviation 0.281 (Fig. 6b). Figure 11(b) shows the distribution of damage factor. When partitioned on web, the average damage factor is 0.0318; comparison, when partitioned along the rib this factor is slightly smaller at 0.0285 (Fig. 7b), i.e., the forming quality of component is better. Partitioned on web, the regions with large damage factor lie in the transitional zone and transverse ribs. The reason is that burring and folding are more prone to occur in transitional zones and rib-piercing occurs in transverse ribs. Therefore in general, the positioning of the partition has little effect on the global deformation, while the damage factor is smaller when partitioned along the rib and hence the forming quality can be improved.

6.2 Effects of Partition Positioning

According to the partition boundary line relative to the position of rib, the boundary line can be set on the left, right, or center of the rib, as shown, respectively, in Fig. 12.

Figure 13 shows the distribution of equivalent strain when the boundary line is set on different positions of the rib. When partitioned on the right of the rib, the average equivalent strain is 0.821 with standard deviation of 0.263 (Fig. 13a). When partitioned on the left of the rib, the average equivalent strain is 0.866 with standard deviation of 0.292 (Fig. 13b), while partitioning in the center of the rib, the average equivalent strain is 0.842 and standard deviation is 0.281 (Fig. 6b). When

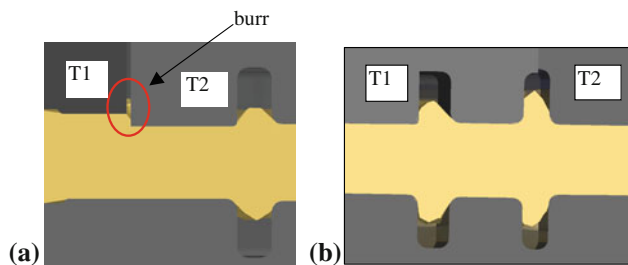


Fig. 10 Forming result of transitional region under different partition modes: (a) partition on web and (b) partition along the rib

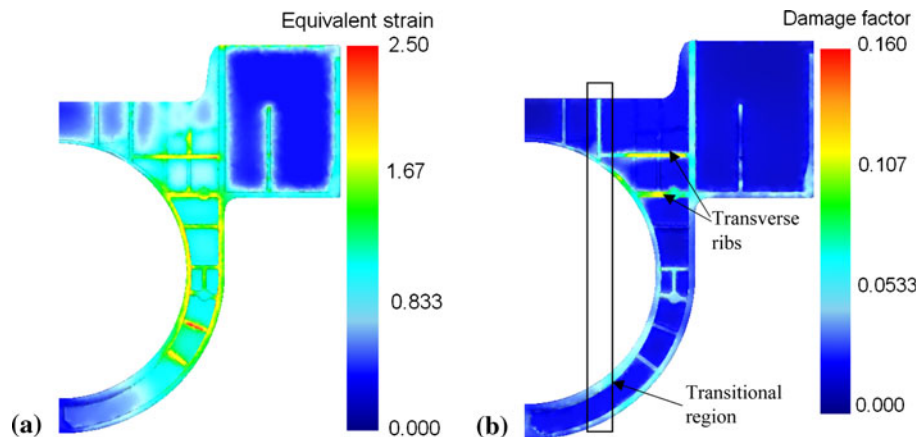


Fig. 11 Forming results when partitioned on web: (a) equivalent strain and (b) damage factor

partitioned on the right of the rib, global deformation is at a maximum and uniformity is at its poorest.

Figure 14 shows the distribution of the damage factor when the boundary line is set at different positions with respect to the rib. We find that for transverse ribs, the rib used for partitioning and the annular ribs in loading zones, the damage factor is relatively large. When the filling of ribs in the loading zone is almost finished, the transverse flow of metal will lead to rib-piercing under further compression. Along partitioning ribs, the damage factor is relatively large as a result of the shift in unloading zone caused by metal flow within the loading zone. The hard forming region, such as the enclosed region A in Fig. 14(a) composed of transverse and annular ribs, is an independent filling zone as shown in Fig. 14(c). Here, the damage factor is large due to the difficulty in metal flow.

When partitioned on the right of the rib, the average damage factor is 0.0297 (Fig. 14a), on the left it is 0.0274 (Fig. 14b), while in the center it is 0.0285 as seen in Fig. 7(b). Damage of the billet is mainly caused by a shift of unloading zone resulting

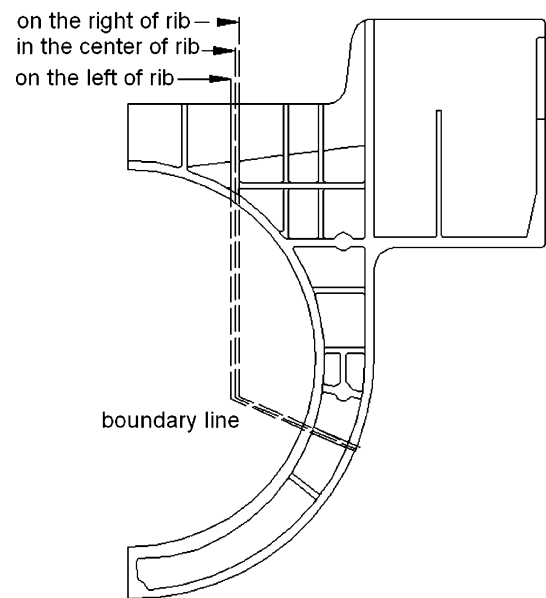


Fig. 12 Schematic diagram of partition position along the rib

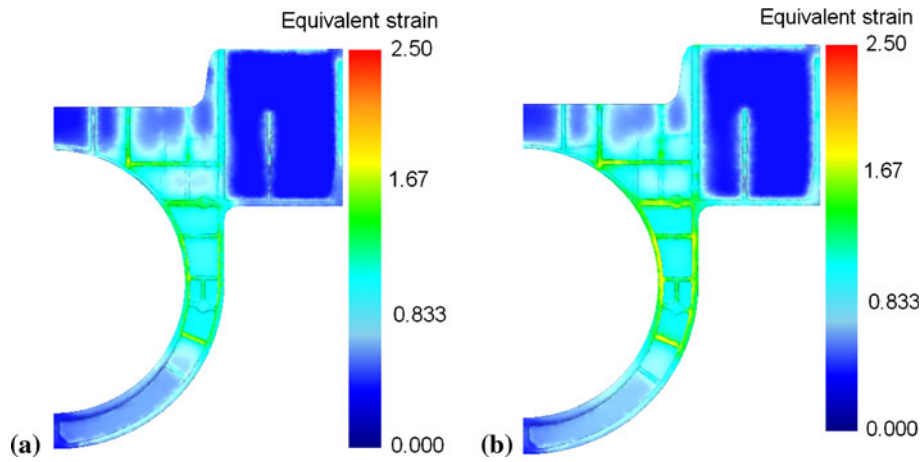


Fig. 13 Distribution of equivalent strain partitioned on different positions of rib: (a) partition on right of rib and (b) partition on left of rib

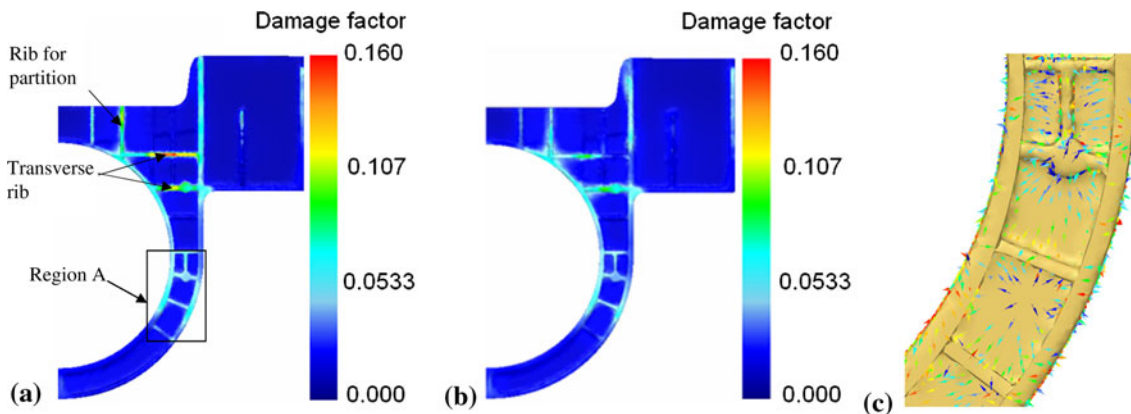


Fig. 14 Distribution of damage factor partitioned on different positions of rib: (a) partition on right of rib, (b) partition on left of rib, and (c) velocity vector of independent filling zone

from metal flowing within the loading zone; when partitioned on the left of the rib, the effect of the shift toward rib-piercing is minimal. With other forming parameters fixed and partitioning is on the left of the rib, rib-piercing defects can be diminished and the fluidity of metal can be improved. Meanwhile, the damage factor is at minimum, and hence partitioning on the left of the rib is recommended.

6.3 Constraint Condition

The constraint of the unloading zone will affect the deformation of the loading zone. Forming defects such as bulging, shifts, and rib-piercing may occur and become severe when the unloading zone is constrained improperly. When other forming parameters given, the effect of constraining the unloading zone is analyzed by setting the constraint clearance to values 0.5, 1, 1.5, and 2 mm. Figure 15 provides distributions of equivalent strain under the various constraint clearances. The results show that with the increase of constraint clearances, the whole deformation and non-uniformity of the billet both decrease.

This is because with small constraint clearance, the area below the constraint die is easily filled by metal from the loading zone. The metal finds difficulty in flowing toward the unloading zone due to the restriction of the constraint die and this will promote deformation of the loading zone. With

increasing the constraint clearance, i.e., weakening restriction, metal flows easily so the whole deformation is more uniform. When the constraint clearance is too large during the first loading step (Top die 1 loaded) more metal flows toward the constraint zone, and during the second loading step (Top die 2 loaded) shifting of metal is large.

Figures 15(c) and 16 show the variation of the damage factor under different constraint clearances. Rib-piercing may occur when the constraint clearance is too small. In short, with increasing constraint clearance, the whole deformation degree of the billet and the non-uniformity of deformation both decrease, however, its effect is not significant. Under forming conditions presented in this article, the possibility of damage is at a minimum when the constraint clearance is 1 mm.

6.4 Effect of Loading Pass

The loading pass will determine the deformation degree in each loading step. If it is not set to a reasonably value, streamline folding will appear and weaken the property and quality of forged parts. For a two-pass loading forming mode, the simulation conditions are as follows: reduction amount per loading pass is 17.0 mm, constraint clearance is 1.0 mm, and for fine deformation the reduction amount is 1.5 mm.

Figure 17 provides distributions of equivalent strain under a two-pass local loading process. Here, the average equivalent

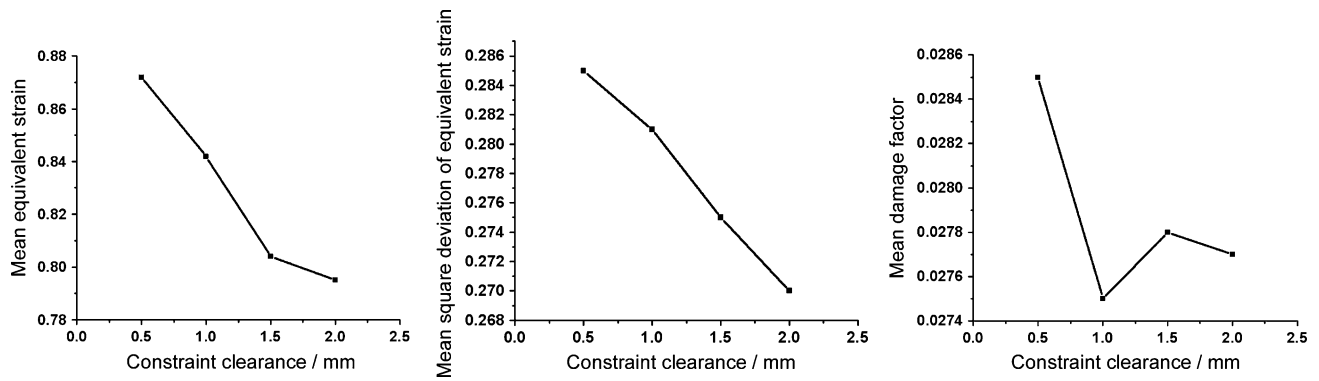


Fig. 15 Variation of equivalent strain and damage factor under different constraint clearances

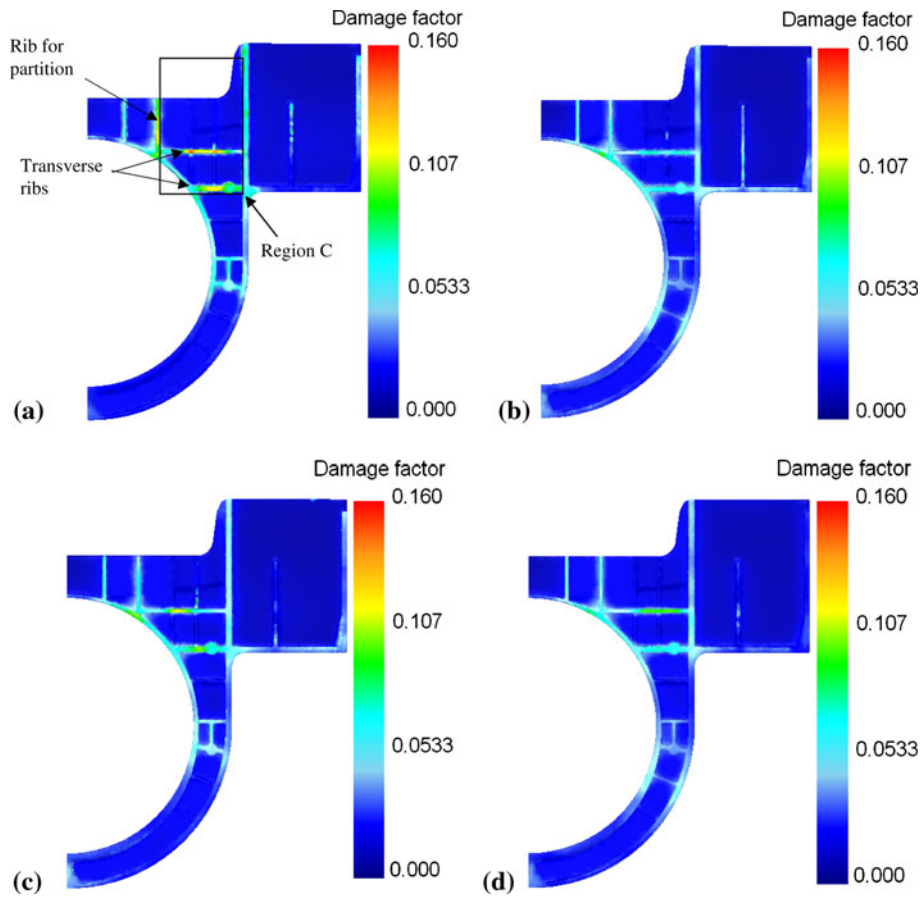


Fig. 16 Distributions of damage factor under different constraint clearances: (a) constraint clearances 0.5 mm, (b) constraint clearances 1 mm, (c) constraint clearances 1.5 mm, and (d) constraint clearances 2 mm

strain is 0.835, with standard deviation of 0.271. Under a single-pass local loading process, the average equivalent strain is 0.842, with standard deviation of 0.281 (Fig. 6b). The loading pass has little effect on the whole deformation, while the deformation is slightly more uniform by using two-pass local loading. After forming, the average of damage factor is 0.027 with two loading passes (Fig. 17b), while it is 0.0285 with a single loading pass, as seen in Fig. 7(b), i.e., the possibility of damage is less using the two-pass local loading mode.

In general, when other forming parameters are kept fixed and comparing single-pass with two-pass local loading, the whole deformation degree increases slightly, and the uniformity of deformation is better with a smaller damage factor. A two-pass local loading process is thus recommended.

All the above analysis shows that for the component studied in this article, the reasonable local loading conditions are as follows: a two-pass local loading mode, partitioning along the rib and on the left of rib, and constraint clearance of 1.0 mm.

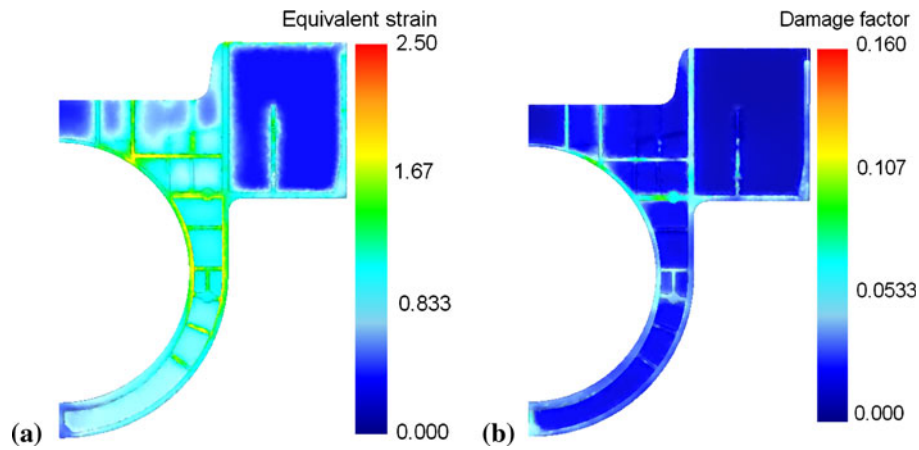


Fig. 17 Distributions of equivalent strain and damage factor under two loading passes: (a) equivalent strain and (b) damage factor

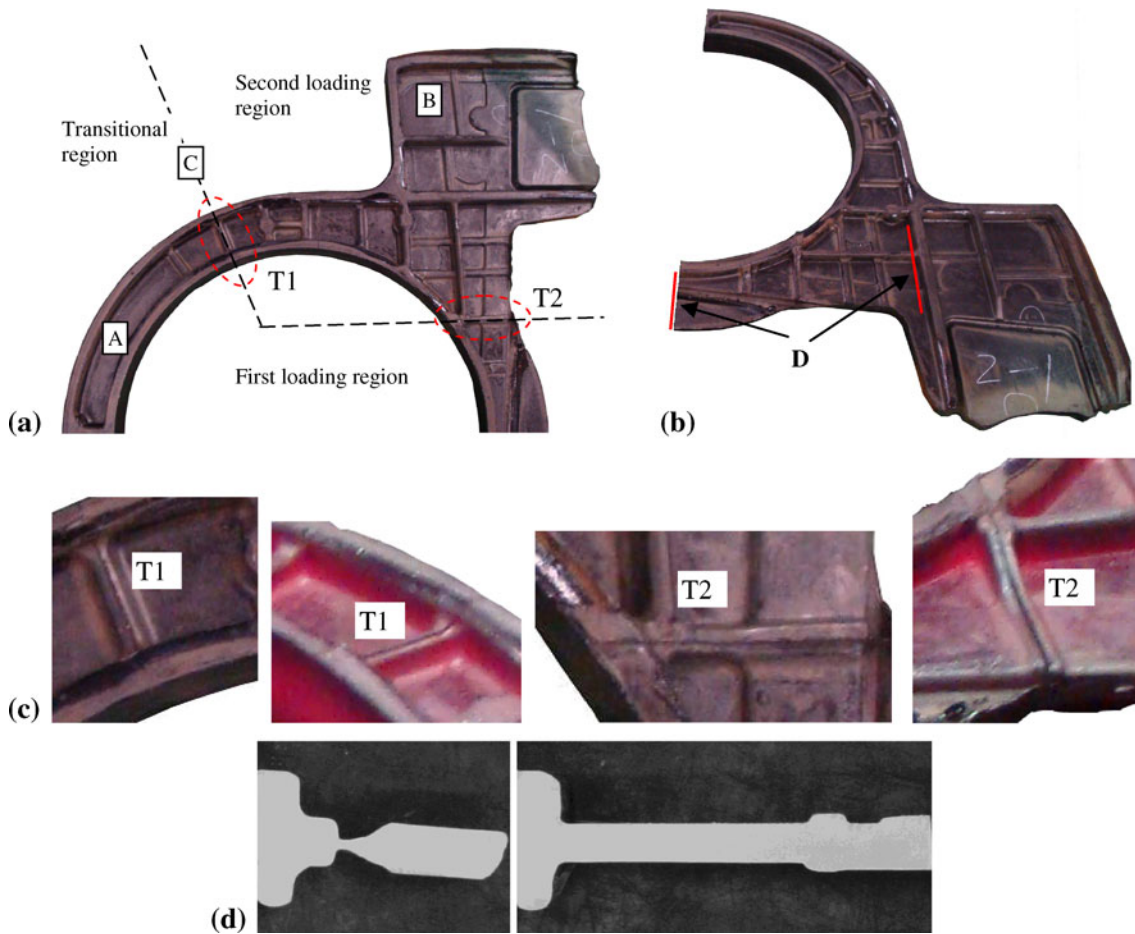


Fig. 18 Photos of TA15 large component formed by local loading. (a, b) the component formed; (c) magnified photos of the transitional regions; and (d) the macrostructures of the component. A, B, C are the corresponding sample locations of microstructure observation for the first-loading region, second-loading region and transitional region. D shows the locations for macrostructure observation; T1 and T2 are the two transitional regions

7. Engineering Practice of TA15 LSRW Component Local Loading Forming

According to the study on local loading process and our former study on the microstructure and mechanical properties of Ti-alloy forging in literature (Ref 11), the forming process of

a typical TA15 component was achieved successfully and the forging with good quality was obtained (shown in Fig. 18) under the following forming conditions recommended through simulation: initial thickness of billet was 50 mm, forming temperature of billet and die was 970°C, loading speed of upper die was 0.1 mm/s, and total reduction amount was 35.5 mm,

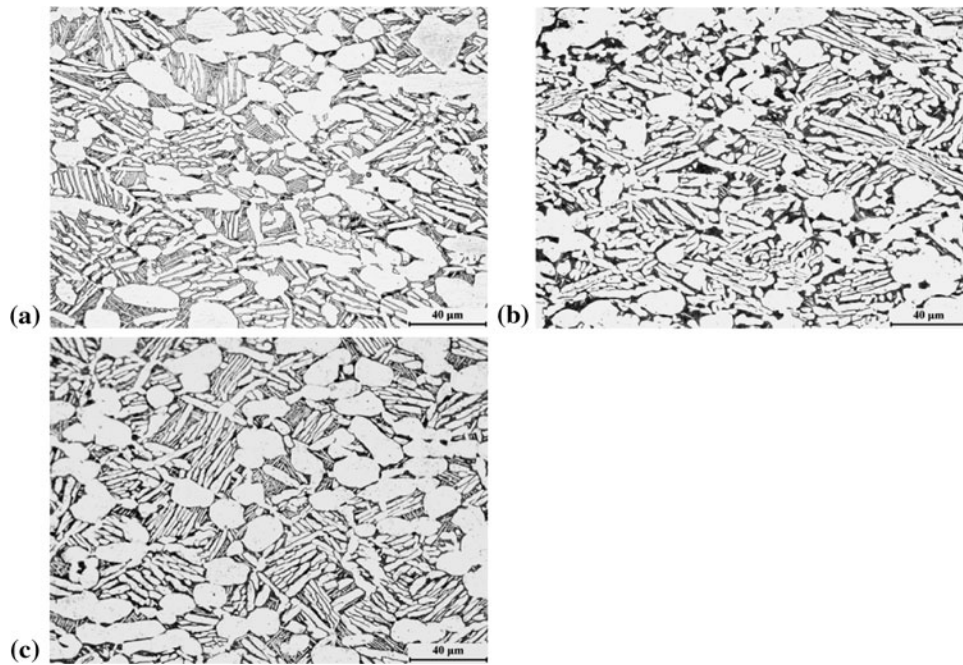


Fig. 19 Metallographic photos of TA15 large component formed by local loading: (a) first-loading region, (b) second-loading region, and (c) transitional region

flashless die forging mode was used and upper die was partitioned along the rib of component, one-pass local loading was adopted, glass-based lubricant was used. No macroscopical forming defects, such as no flow line defect is observed (Fig. 18d) which means the component can satisfy the demands in aircraft domains.

Figure 19 shows metallographic photos of first loading region, second loading region, and transitional region (marked as A, B, C, respectively in Fig. 18a) of formed component, Table 1-3 (Ref 12) provides the mechanical properties of component. The fine microstructure and excellent comprehensive performance which meets the requirement were obtained.

This further indicates the reliability and practical value of results obtained in this article.

8. Conclusions

- (1) For LSRW component ILL forming the “rib-piercing” caused by horizontal flow of metal can be reduced using flashless die forging and the damage factor of forged part is much smaller when compared with open-die forging. As the friction factor increases, the deformation of the billet becomes more uneven.
- (2) Compared with partitioning on the web, the whole material flow capability and forming quality of the transition region can be improved when the loading zone and die are partitioned along the ribs, and the damage factor is much smaller with an improved uniformity of deformation. In detail, when the partition boundary line is on the left of the rib, the “nailing-up” effect of partitioning ribs toward material flow can be reduced and the “rib-piercing” can be diminished, while the damage factor of forming is at a minimum.
- (3) With increasing the constraint clearance, the whole deformation degree of the billet and the non-uniformity

of deformation both decrease, however, its effect is not significant. Under the forming condition studied in this article. The damage factor is at a minimum when the constraint clearance is 1 mm.

- (4) For the component studied in this article, the reasonable local loading conditions were obtained as follows: closed die forging, a two-pass local loading, partitioning along the rib and on the left of rib, and a constraint clearance of 1.0 mm.
- (5) According to the simulation results the practical forming of TA15 LSRW component was achieved successfully and the forging with good forming quality, fine microstructure and excellent comprehensive mechanical properties which meets the requirement were obtained.

The results obtained provide a basis for optimizing the forming process and priming a parameter selection for better complex LSRW component ILL forming.

Acknowledgments

The authors would like to gratefully acknowledge the support of Natural Science Foundation for Key Program of China (50735005, 50935007), Natural Science Foundation (50905145), National Basic Research Program of China (2010CB731701), the 111 Project (B08040) and fund of the State Key Laboratory of Solidification Processing in NWPU (59-TP-2010).

References

1. G.H. Shen and D. Furrer, Manufacturing of Aerospace Forgings, *J. Mater. Process. Technol.*, 2000, **98**, p 189–194
2. S.H. Zhang, Z.R. Wang, Z.T. Wang et al., Some New Features in the Development of Metal Forming Technology, *J. Mater. Process. Technol.*, 2004, **151**, p 39–47

3. Z.C. Sun and H. Yang, Mechanism of Unequal Deformation During Large-Scale Complex Integral Component Isothermal Local Loading Forming, *Steel Res. Int. Sp. Ed.*, 2008, **79**(1), p 601–608
4. B. Claudior, Process Modeling of Forming of Structural Parts With Thin Ribs, *J. Mater. Process. Technol.*, 1984, **26**, p 337–349
5. Z.C. Sun and H. Yang, Analysis on Process and Forming Defects of Large-Scale Complex Integral Component Isothermal Local Loading, *Mater. Sci. Forum*, 2009, **614**, p 117–122
6. Z.C. Sun and H. Yang, Forming Quality of Titanium Alloy Large-Scale Integral Components Isothermal Local Loading, *Arab. J. Sci. Eng. (AJSE)*, 2009, **34**(1), p 35–45
7. K.J. Vinod, L.G. Robert, and M.L. Carl, Application of Computer Methods to the Design and Analysis of Precision Rib-Web Forgings, *J. Mater. Process. Technol.*, 1992, **36**, p 1–16
8. Y.G. Zhou, W.D. Zeng, and H.Q. Yu, An Investigation of a New Near-Beta Forging Process for Titanium Alloys and its Application in Aviation Components, *Mater. Sci. Eng. A*, 2005, **393**, p 204–212
9. Z.M. Hu, J.W. Brooks, and T.A. Dean, Experimental and Theoretical Analysis of Deformation and Microstructural Evolution in the Hot-Die Forging of Titanium Alloy Aerofoil Sections, *J. Mater. Process. Technol.*, 1999, **88**, p 251–265
10. N.G. Sun, H. Yang, and Z.C. Sun, Optimization on the Technical Process of Large Titanium Bulkhead Isothermal Closed-Die Forging, *Rare Met. Mater. Eng.*, 2009, **38**(7), p 1296–1300 (in Chinese)
11. Z.C. Sun and H. Yang, Microstructure and Mechanical Properties of TA15 Titanium Alloy Under Multi-Step Local Loading Forming, *Mater. Sci. Eng. A*, 2009, **523**, p 184–192
12. X. Fan, He Yang, Z. Sun, and D.W. Zhang, Effect of Deformation Inhomogeneity on the Microstructure and Mechanical Properties of Largescale Rib-Web Component of Titanium Alloy Under Local Loading Forming, *Mater. Sci. Eng. A*, 2010, **527**, p 5391–5399
13. C.W. Shen, Research on Material Constitution Models of TA15 and TC11 Titanium Alloys in Hot Deformation Process, Master Thesis, Northwestern Polytechnical University, Xi'an, 2007
14. F.A. McClintock, A Criterion for Ductile Fracture by the Growth of Holes, *J. Appl. Mech.*, 1968, **6**, p 363–373
15. S.L. Semiatin, R.T. Goetz, E.B. Shell et al., Cavitation and Failure During Hot Forging of Ti-6Al-4V, *Metall. Mater. Trans. A*, 1999, **30**, p 1411–1424